Finansējuma saņēmēja nosaukums
Latvijas Universitāte

Īstenotā projekta nosaukums
„Jaunas matemātiskās modelēšanas instrumentu sistēmas izstrāde funkcionālo nano- un mikroelektronikas pusvadītāju materiālu ražošanas tehnoloģijām"

Īstenotā projekta Nr.
2011/0002/2DP/2.1.1.1.0/10/APIA/VIAA/085

Projekta LU reģistrācijas Nr.
ESS2011/121

Projekta zinātniskais vadītājs
Dr.-Phys., Jānis Virbulis

Tehniskā atskaite

par 3. aktivitāti:

Nanomērogu procesu modelēšanas rezultātu vidējošanas metodikas izstrāde, sagatavojot lokālas parametrizētus nepārtrauktas vides sakarības makroskopiskajiem modeļiem; atbilstošo skaitlisko metožu izstrāde

Rīga, 2013

1 Ievads

Aktivitātes mērķis projekta ietvaros ir izveidot papildinājumu ar nanomērogu, kinētiskiem un mikroskopiskiem modeļiem matemātiskās modelēšanas un programmu bāzes sistēmai (MMPBS), kas tiek izmantota funkcionālo un pusvadītāju materiālu ražošanas tehnoloģiju matemātiskajā modelēšanā un kas ir izstrādāta un implementēta programmu kompleksa veidā uz Fizikas un Matemātikas Fakultātes daudzprocesoru klastera. Tas ļauj analizēt gan tehnoloģisko procesu makroskopiskos, gan nanomērogu, kinētiskos un mikroskopiskos procesus, gan to saistību.
Šīs atskaites plāns ir sekojošs, otrajā atskaites sadaļā formulēta risināmā problēma, apkopotas iepriekšējās zināšanas un ieviesti izmantojamie apzīmējumi. Trešā sadaļa apraksta molekulārās dinamikas aprēķinus. Pēdējā sadaļa apraksta leņķisko Voronkova diagrammu iegūšanu un iegūtas diagrammas nozīmīgumu silīcija kristāla audzēšanai. Visas šīs atskaites daļas ir angļu valodā.

2 Growth of monocrystalline silicon from a melt

Growing monocrystalline silicon from a melt, a variety of distinguishing features may appear on otherwise smooth external surface of a cylindrical crystal, Figure 1. Depending on their appearance they have been called as ridges [**Error! Reference source not found.**], protrusions [Fritzler et al.Fritzler, Trukhanov, Kalinin, Smirnov, Kolesnikov, and Vasilenko], growth lines [**Error! Reference source not found.**], bulges [**Error! Reference source not found.**], projections [**Error! Reference source not found.**], etc, but they all can be described by the same growth mechanism. The theoretical description of these structures had been developed by V. V. Voronkov around the year 1980 [**Error! Reference source not found.**, **Error! Reference source not found.**, **Error! Reference source not found.**]. The description relies on the analysis of the interface free energies and on a model of curvature driven atomic diffusion along the crystal external surface.

Figure 1 The growth mechanisms at the atomic scale can visibly affect the single crystal surface shape at macroscale

Knowledge of all interface energies allows one to solve Herring's equation [**Error! Reference source not found.**] for the equilibrium orientation of interfaces at the at the triple phase line (TPL)

$$\sum_i(\gamma_i e_i + \gamma_i' e_i^+) = 0, \qquad (1)$$

where e_i are unit vectors parallel to interface i at the TPL, but e_i^+ are unit vectors perpendicular to e_i, Fig. 2. The sum i is over all three interfaces and γ_i' is derivative with respect to an angular coordinate.

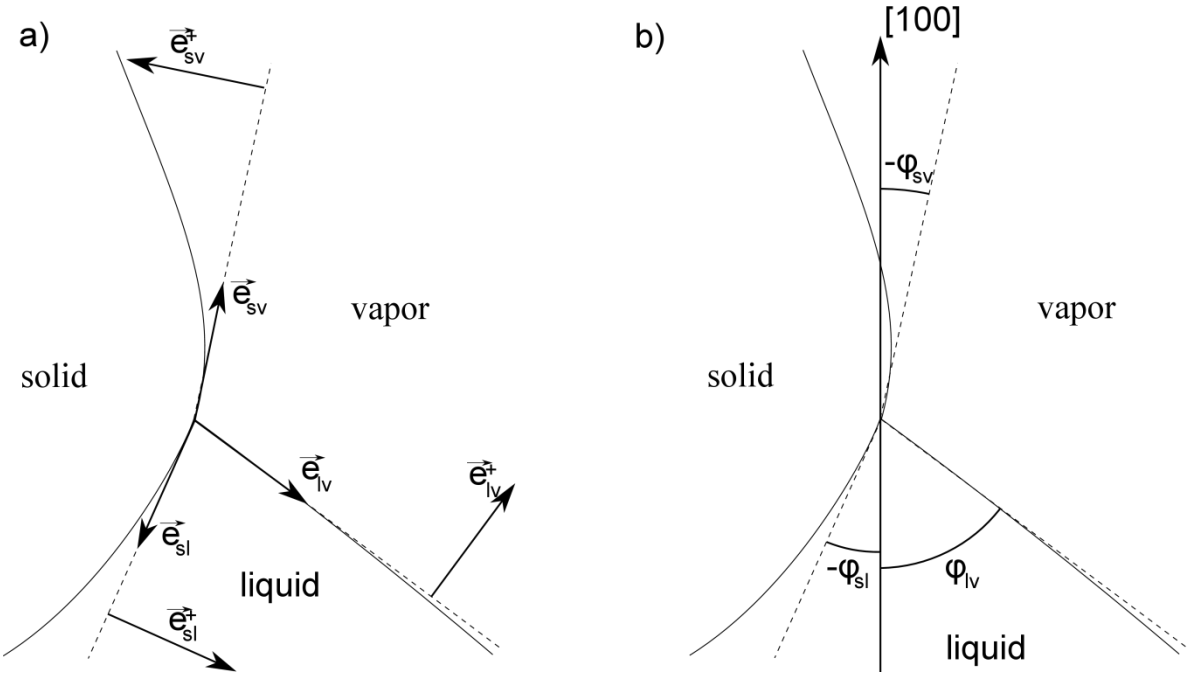

Figure 1: a) The orientation of unit vectors at the triple point. "sv" stands for solid-vapor interface, "lv" for liquid vapor, "sl" for solid liquid. b) The angles are measured at TPL in liquid-vapor-solid direction between [100] axis and tangent to the interface. In order to simplify relevant equations and angular diagrams, the angle for solid-vapor interface is measured from the opposite end of the [100] axis than angles for melt interfaces

The equation can be solved graphically as an intermediate step using Wulff's construction, Fig. 2. The first step in Wulff's construction is to draw the interface energies in a polar γ plot. The inner envelope, Γ_i, of planes perpendicular to radius-vectors is geometrically similar to the equilibrium shape of the interface [**Error! Reference source not found.**].

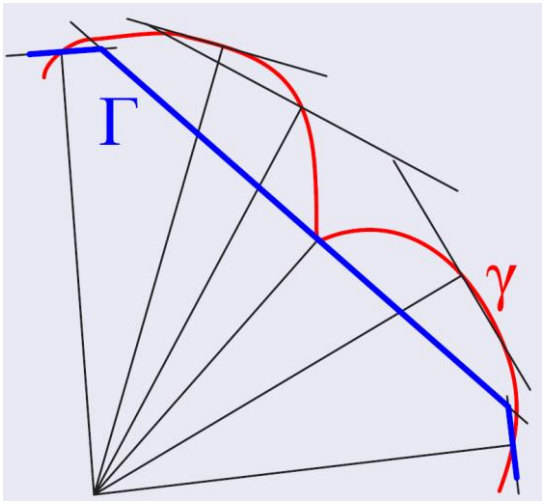

Figure 2. Wulff construction

The inner envelopes for three interfaces, Γ_{sv}, Γ_{sl} and Γ_{lv}, can be used to find equilibrium orientation of the crystal external surface (crystal-vapor interface), the internal surface (crystal-melt interface) and the free melt surface at the TPL [**Error! Reference source not found.**]. The solution is represented as a plot, angular Voronkov diagram, which shows the equilibrium orientation of external and internal crystal surfaces as functions of the free melt surface angle. From the diagram we can find the dependence of the growth angle on the crystallographic orientation, as well as the orientations of free melt surface leading growth of {111} facets on the crystal internal or external surface.

The second element of Voronkov's theory is the model of the curvature driven atomic diffusion. It predicts for an undercooled melt that due to the atomic diffusion of melt atoms, the observed orientation of external surface can differ considerably from the equilibrium orientation found from the free energies above. The diffusion is directed along crystal external surface away from the TPL. The undercooling is explained by lower temperatures needed for the growth of an internal {111} facet, growing by 2D nucleations, in comparison to the rest of the crystallization front growing by rough growth. Whenever the {111} internal facet appears close to the TPL, the macroscopical growth angle will be different from the growth angle in immediate vicinity of the triple point due to mass transport at nanoscale, Fig. 4 and 5. This results in a macroscopically visible structure on the external crystal surface. The difference between the macroscopically observed growth angle ε^* and the growth angle at TPL, ε, given by equilibrium orientation of interfaces is [**Error! Reference source not found.**]

$$\epsilon^* - \epsilon = -C v_p^{-1/3} \Delta T, \qquad (2)$$

where v_p is crystal pulling speed, $\Delta T = T_m - T$ is the undercooling of melt below the crystal melting temperature T_m, and C is a coefficient that depends on material constants and temperature of the melt, T.

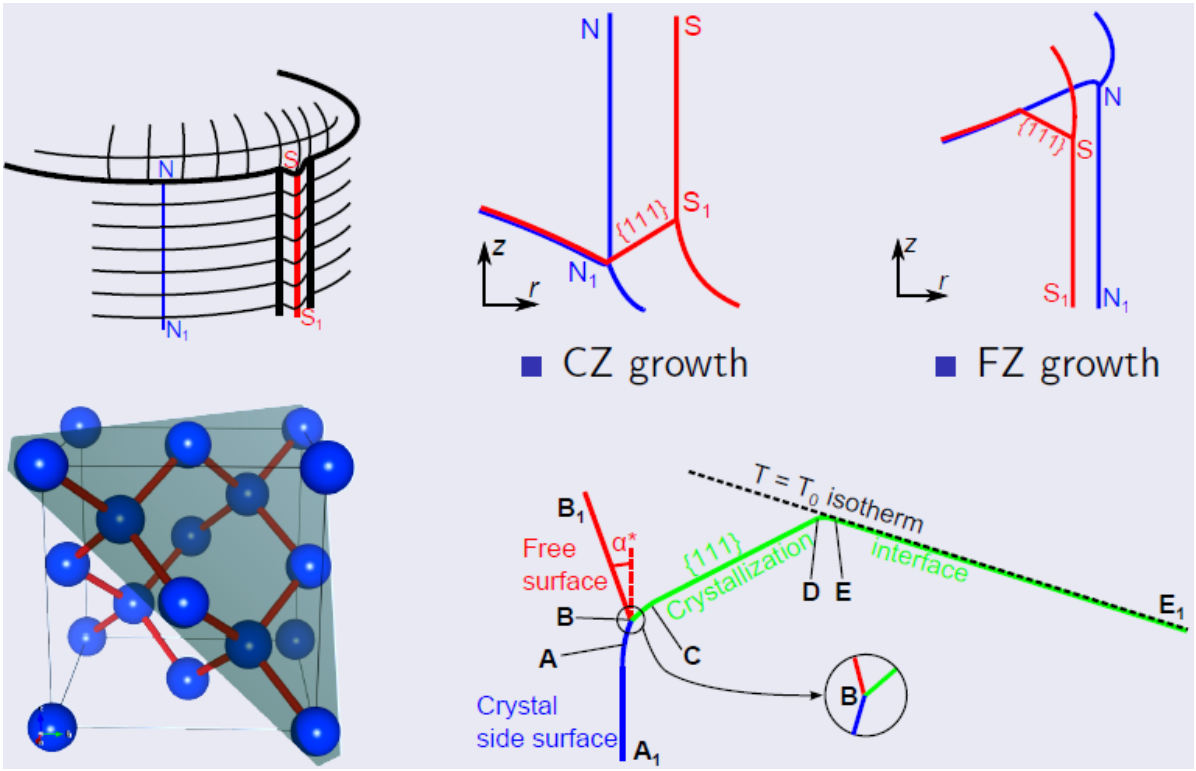

Figure 4. The undercooling is explained by lower temperatures needed for the growth of an internal {111} facet, growing by 2D nucleations, in comparison to the rest of the crystallization front growing by rough growth.

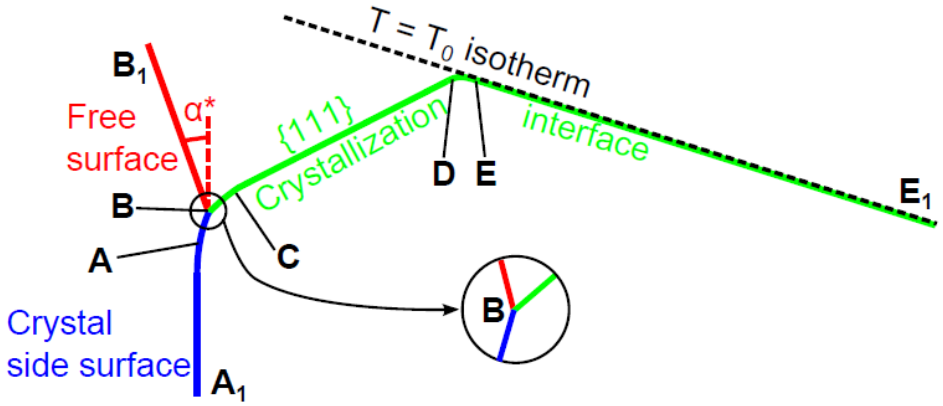

Figure 5. AA1 a fully developed crystal lateral surface. Voronkov theory; AB a curved part of lateral surface. Voronkov theory; BC a curved part of crystallization interface in direct vicinity of triple phase line. Curvature and undercooling of the front is connected by Gibbs-Thomson equation; CD a {1 1 1} facet, practically flat. Significant undercooling of the order of 4 K; DE a curved part of crystallization interface. Undercooling below 0.1 K. Gibbs-Thomson equation; EE_1 a part of the crystallization interface. Undercooling of few mK. It closely follows $T = T_0$ isotherm. It is determined by macroscopic temperature field; BB_1 a free surface of liquid determined by such physical effects as hydrostatic and EM pressure, as well as centrifugal forces due to rotation of the liquid. The orientation of the interfaces at triple phase line (B) is determined by Herring equation

For silicon the model of Voronkov depends on several little known physical parameters and so far the description has been used to make qualitative ad hoc predictions for silicon crystal growth. Such an approach does not uses the full predictive power of the Voronkov model where the same description could be universally applied for different crystallographic

orientations of growing crystals (e.g. <100>, <111>), for growth of crystals of different sizes (e.g. macroscopic or microscopic crystals), for different methods of crystal growth (e.g. Float zone or Czochralski) and, possibly, prove or disprove the validity of Voronkov's approach or show its limits of applicability. In this paper we will show that angular Voronkov diagrams could be obtained using molecular dynamics studies. An advantage of this approach in comparison to ad hoc construction of the diagrams is that it is universal for the different types of silicon crystal growth. Another advantage is that the description could by systematically improved by more accurate numerical studies.

2 Molecular dynamics simulations

The values of the interface energies and their derivatives in Eq. 1 are physical parameters that have proved to be difficult to obtain from experiments. This is especially true for the crystal-melt interface, which is hidden for external observers. In order to have the melt, the temperature of a system should be above the melting temperature and for silicon that leads to a harsh experimental environment. On the contrary numerical modeling, for example by molecular dynamics, allows easily to visualize processes at the internal surface and to change the temperature of the system simply. Still, the derivation of the angular dependence of interface energies by molecular dynamics approach is a challenging and time-consuming task.

The experimental study of equilibrium shape of silicon nanoparticles at 1373 ^{o}K have been presented in Ref. [Muller and Metois] and for the shape of nanocavities at 973 ^{o}K in Ref. [Eaglesham et al.Eaglesham, White, Feldman, Moriya, and Jacobson], Fig. 6. Even noting the different temperatures, the obtained discrepancies of interface energies in these two studies seem to be irreconcilable, justifying further study.

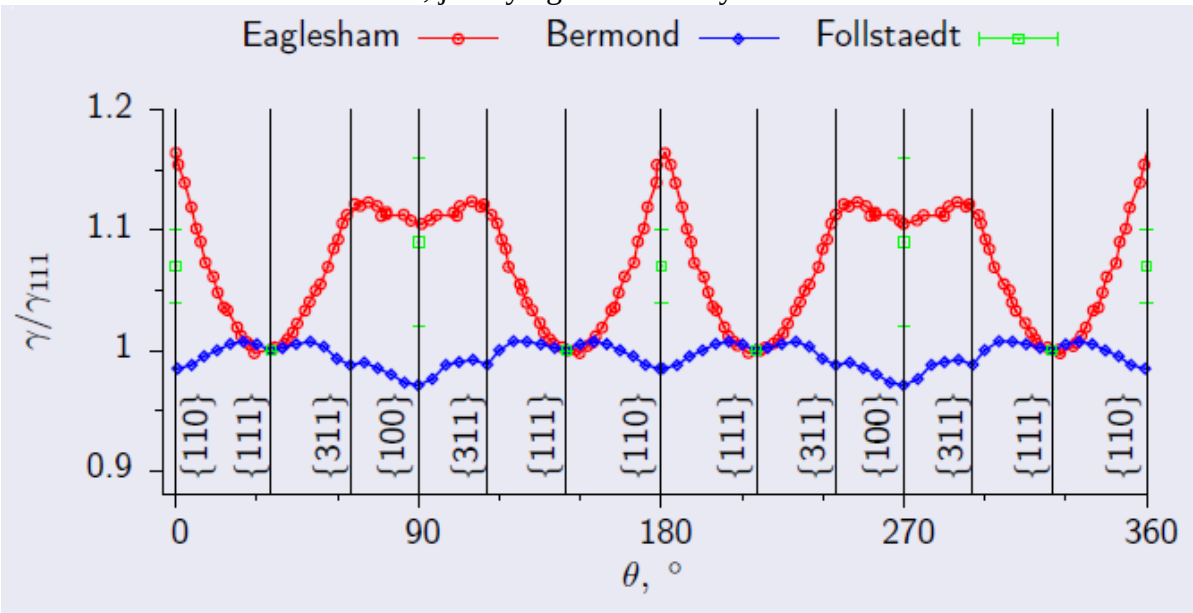

Figure 6. Discrepancies among surface energies obtained by various experimental studies.

To model the equilibrium shape of crystalline silicon, we did molecular dynamics simulations using LAMMPS, a parallel classical molecular dynamics simulation code [Plimpton]. The Stillinger-Weber three-body potential [Stillinger and Weber], Fig. 7, which allows to account for tetrahedral structure of silicon crystal, was used.

$$V = \sum_{\substack{i,j \\ i<j}} \varepsilon\, f_2\left(\frac{r_i}{\sigma}\right) + \sum_{\substack{i,j,k \\ i<j<k}} \varepsilon\, f_3\left(\frac{\boldsymbol{r}_i}{\sigma}, \frac{\boldsymbol{r}_j}{\sigma}, \frac{\boldsymbol{r}_k}{\sigma}\right)$$

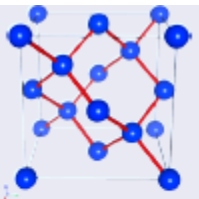

$$f_2(r) = \begin{cases} A\left(\frac{B}{r^p} - \frac{1}{r^q}\right)\exp\left[\frac{1}{r-a}\right], & r < a \\ 0, & r \geq a \end{cases}$$

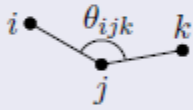

$$f_3(\boldsymbol{r}_i, \boldsymbol{r}_j, \boldsymbol{r}_k) = h(i,j,k) + h(j,i,k) + h(k,i,j)$$

$$h(i,j,k) = \begin{cases} \lambda \exp\left[\frac{\gamma}{r_{ij}-a} + \frac{\gamma}{r_{ik}-a}\right]\left(\cos\theta_{jik} + \frac{1}{3}\right)^2, & r_{ij}, r_{ik} < a \\ 0 & \text{otherwise} \end{cases}$$

$A = 7.0495,\ B = 0.60222,\ p = 4,\ q = 0,\ a = 1.80,\ \lambda = 21.0,\ \gamma = 1.20$

Figure 7. Parameters used to describe Stillinger-Weber three-body potential

Starting from an arbitrary initial crystalline system bellow melting temperature and waiting for sufficiently long time, the shape of the system should approach the equilibrium shape. However, the time to reach the equilibrium shape might be too long for practical purposes. Taking into account the small time step of molecular dynamics calculations, around 1 femtosecond, it is not always possible to reach the equilibrium shape in a calculation. In order to reach the equilibrium shape, it is useful to choose the shape of initial system close to the equilibrium shape. Since anisotropy of interface energy decreases approaching the melting temperature, a spherical shape could be good guess for the initial shape of a particle close to the melting temperature.

Much of the relevant information about crystal growth, including the angular diagrams, can be obtained from 2D cross-sections of the equilibrium shapes. Cylindrical initial system with infinite curvature radius in the direction perpendicular to the cross-section, allows us to reduce the calculation to basically 2D case. In our calculations the initial cylindrical system contained about 3500 atoms with the cross-section of about 7.6 nm in diameter. In the axial [-110] direction periodic boundary conditions were used. The width of the periodic slab was about 1.5 nm. To accelerate calculations, the atoms in the center of the nanoparticle were fixed at their initial positions. This central part had a radius of about 1.5 nanometers.

At temperatures close to the melting temperature the shape of the system will be disturbed by atomic fluctuations. Higher temperatures facilitate atomic diffusion decreasing calculation time. In order to faster approach the equilibrium shape, the temperature of the outer layer initially was risen to 2300 K until it melted, then the temperature was lowered to 1605 K in order to allow crystallization. When the system have crystallized, the temperature was kept approximately constant by Langevin thermostat at 1605 K only in 0.8 nm thick layer surrounding the central part of the fixed atoms. The atoms in outer layer, about 1.5 nanometers thick, moved without the thermostat in order not to affect the atomic diffusion on the surface of the particle [Weakliem and Carter].

We have made several calculations and followed the shape of the silicon crystal. We were looking for the shape of cross-section that would have D_{2h} symmetry and would not change with time in order to predict whether the system has reached the equilibrium shape at a given temperature.

A snapshot of a calculation with such symmetric shape is shown on Fig. 7. The shape of the nanoparticle is similar to the shape of nanocavities obtained by Eaglesham et al [Eaglesham et al.Eaglesham, White, Feldman, Moriya, and Jacobson] and shown on Fig. 8. The agreement between the experimental and theoretical shapes is very good, although in the experiment the shape is obtained at lower temperatures. Assuming that the interface free

energy does not depend on the interface curvature, both the cavity and nanoparticle are described by the same γ plot and have the same equilibrium shape.

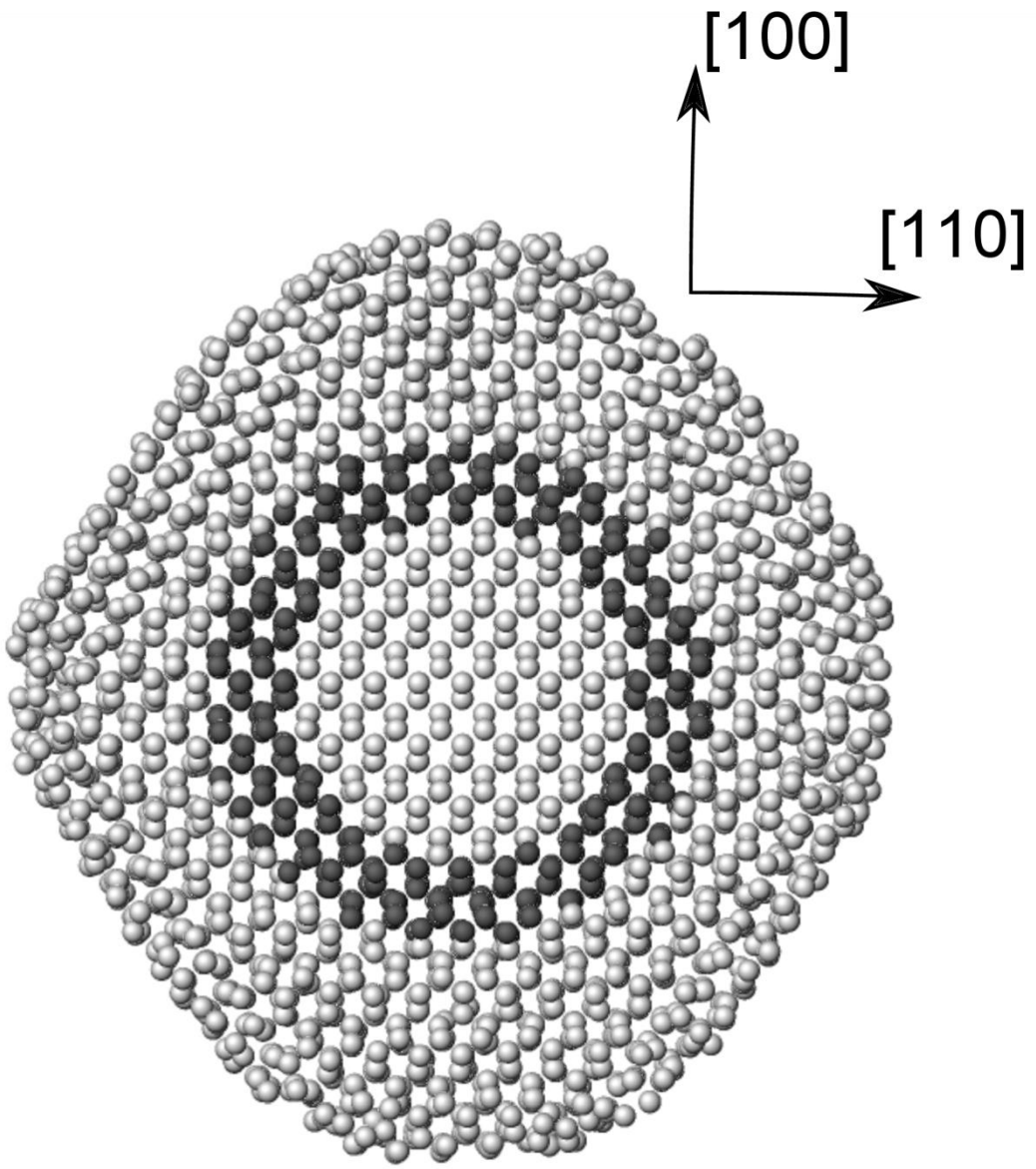

Figure 7: The shape of silicon crystal calculated by molecular dynamics calculation is approximately symmetric and shows well pronounced {111} facets on the external surface. The system is about 7.6 nm wide. Darker ring shows the part of the system where thermostat is applied. The atoms in inner part are fixed during calculation. The shape is obtained after 83 ns calculation

The both surfaces show well pronounced {111} facets and considerable rounding of the interface in <100> directions. Rounded part of the interface in <110> direction is much smaller. This is clearly visible for the experimental shape, whereas for the theoretical it is difficult to make definite conclusions about the rounding due to the significant size of interatomic separation in comparison to the size of the corners and also due to the atomic fluctuations.

In Ref. [Eaglesham et al.Eaglesham, White, Feldman, Moriya, and Jacobson] it was argued that since the experimentally observed equilibrium shape has no sharp corners, then the Wulff construction can be reversed and γ plot giving relative values of interface free

energies for different orientations could be obtained. Looking at the theoretical equilibrium shape, we can not exclude the existence of sharp corners near {111} facets. To make a definite conclusion, calculations for considerably larger systems have to be done. Nevertheless, based on the theoretical grounds we know that the calculated shape is geometrically similar to the Wulff form, Γ_{sv} and this information is sufficient to construct the angular Voronkov diagram.

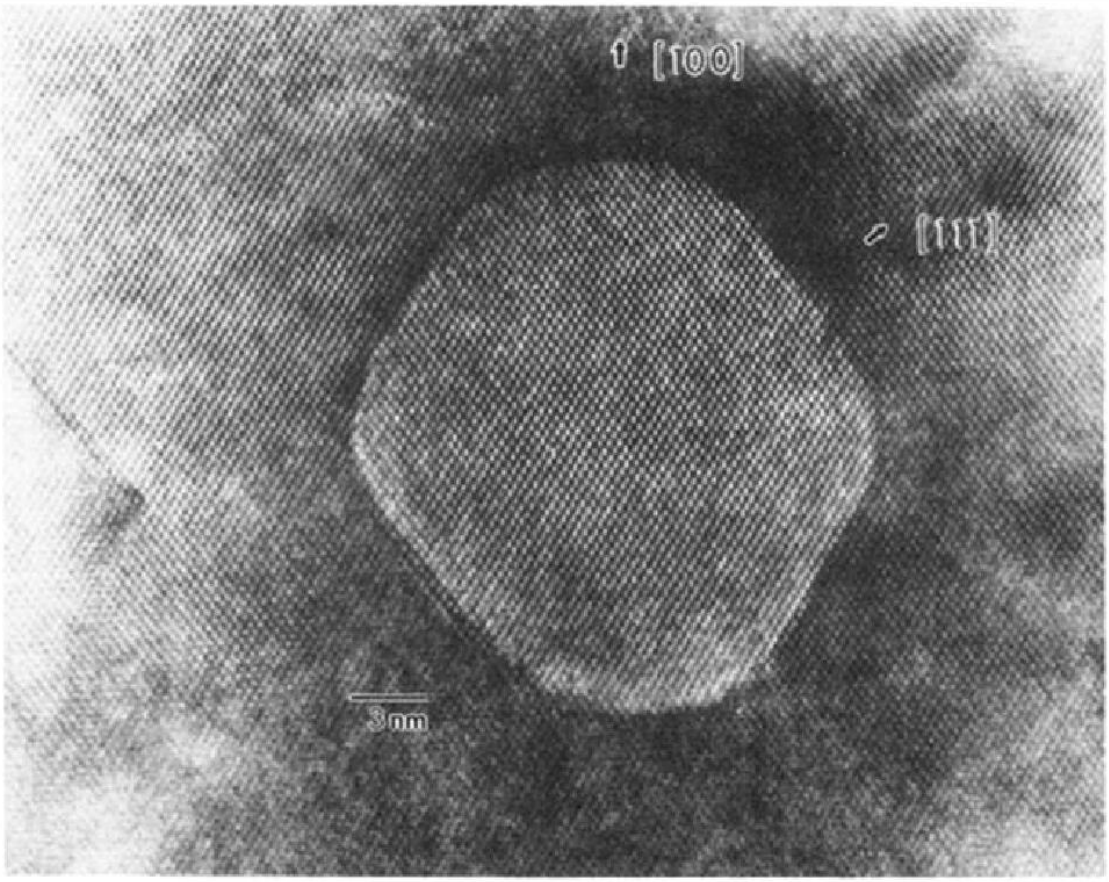

Figure 8: The photo shows annealed void in crystalline silicon. Flat {111} facets are clearly visible. The void is about 20 nm wide. Reproduced from [Eaglesham et al.Eaglesham, White, Feldman, Moriya, and Jacobson]

3 Angular Voronkov diagram

Relying on the agreement between the experimental data [Eaglesham et al.Eaglesham, White, Feldman, Moriya, and Jacobson] and our calculations, we constructed the angular Voronkov diagram [**Error! Reference source not found.**]. We used the equilibrium shape for crystal-vapor interface predicted from our molecular dynamics calculation. In order to minimize the effect of atomic fluctuations at nonzero temperature, the shape of the surface have been averaged over 4 ns simulation starting from the shape shown on Fig. **Error! Reference source not found.**. Over this time period the surface retains the symmetric shape. The averaged shape was fitted assuming that the interface in <100> and <110> direction is round, but in <111> directions flat facets formed. The three fitting parameters corresponding to the interface energies in <100>, <110> and <111> low-index directions were found. In

order to set the scale, the value of γ_{100} was chosen to be equal to 1.2 J/m^2. That brings the fitted value of γ_{111}=1.05±0.03 J/m^2 in close agreement to the value γ_{111}=1.08±0.03 J/m^2 at 1683 K given in Ref. [Scheel and Fukuda]. The last fitting parameter is γ_{110}=1.17±0.03 J/m^2. The approximation error shows the maximal deviation of the fit from the averaged shape found from the molecular dynamics calculation. For the internal surface the same assumptions about the shape of the solid-melt interface as for external surface were used with γ_{100}=0.42±0.02 J/m^2, γ_{111}=0.34±0.02 J/m^2, γ_{110}=0.35±0.03 J/m^2 taken from Ref. [Apte and Zeng]. For free melt surface γ_{sl}=0.83 J/m^2 was used [Eustathopoulos et al.Eustathopoulos, Nicholas, and Drevet].

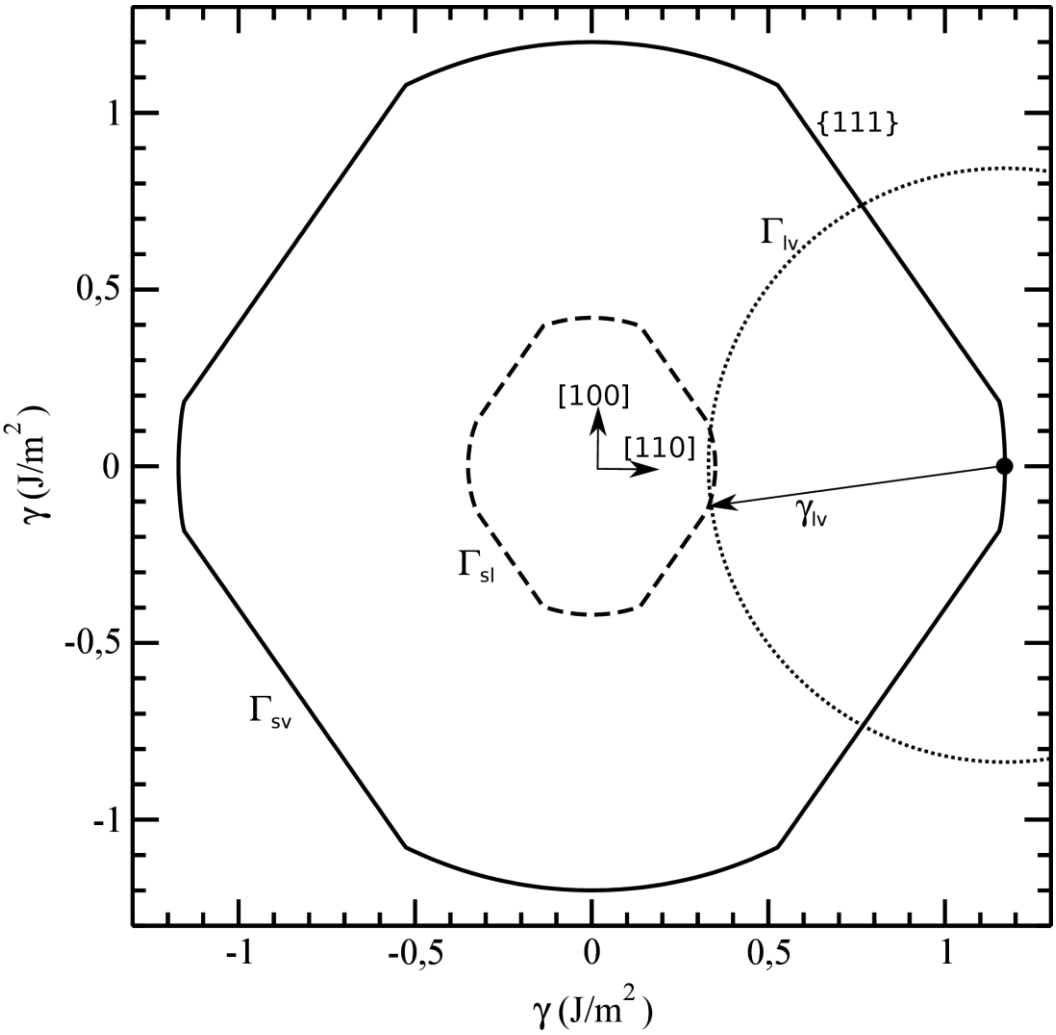

Figure 9: Geometric construction in order to obtain the equilibrium orientation of external and internal crystal surface depending on orientation of the free melt surface. Solid line shows equilibrium shape of solid-vapor interface Γ_{sv}, dashed line models solid-liquid interface Γ_{sl} and dotted line shows shape of equilibrium liquid-vapor interface Γ_{lv}. Γ_{sl} and Γ_{sv} could be obtained from the unknown dependence of interface free energies on crystallographic orientation

The procedure to obtain the angular diagram, Ref. [**Error! Reference source not found.**], is as follows. First, equilibrium shapes for crystal external and internal surfaces are drawn with a common center. The scale is such that the length of radius vector in low-index direction is

equal to the corresponding low-index interface free energy. For a freely chosen point on the Γ_{sv} surface, the tangent of Γ_{sv} at this point will be equilibrium orientation of the solid-vapor surface. Next, circle Γ_{lv} with radius γ_{lv} is plotted from this point and its crossing with Γ_{sl} is found, see Fig. 9. Then the equilibrium orientation of internal surface is tangent to the Γ_{sl} at its crossing with Γ_{lv} for the melt orientation tangent to the Γ_{lv} at this point.

Repeating the procedure for different initial points on the external surface Γ_{sv}, the dependence of orientation of the crystal external and internal surfaces on the free melt surface angle were obtained, see Fig. 10. The obtained curves describing the orientation of the crystal interfaces are rather smooth and have discontinuities only on the appearance of {111} facets. We see that the growth angle has small positive value for a wide range of melt angles. The calculated growth angle $\varepsilon=\phi_{lv}-\phi_{sv}$ for <100> growth is 10^{o}. That is close to the value of 11^{o} determined by several studies [**Error! Reference source not found.**, **Error! Reference source not found.**, **Error! Reference source not found.**]. The agreement further justifies the choice of the scaling used for γ_{sv}.

Analyzing the effect of uncertainties of the γ_i values on the angular Voronkov diagram, we observe that equilibrium orientation of external surface $\phi_{sv}(\phi_{lv})$ is weakly sensitive to changes of the γ values. In comparison, the orientation of the internal surface can change significantly by changing the γ_i values by just a few percents. This is explained by the values of interface energies that happen to be such that Γ_{lv} in Fig. 9 just touches Γ_{sl} figure and small changes in the values of interface energies can change the crossing point of the two figures considerably.

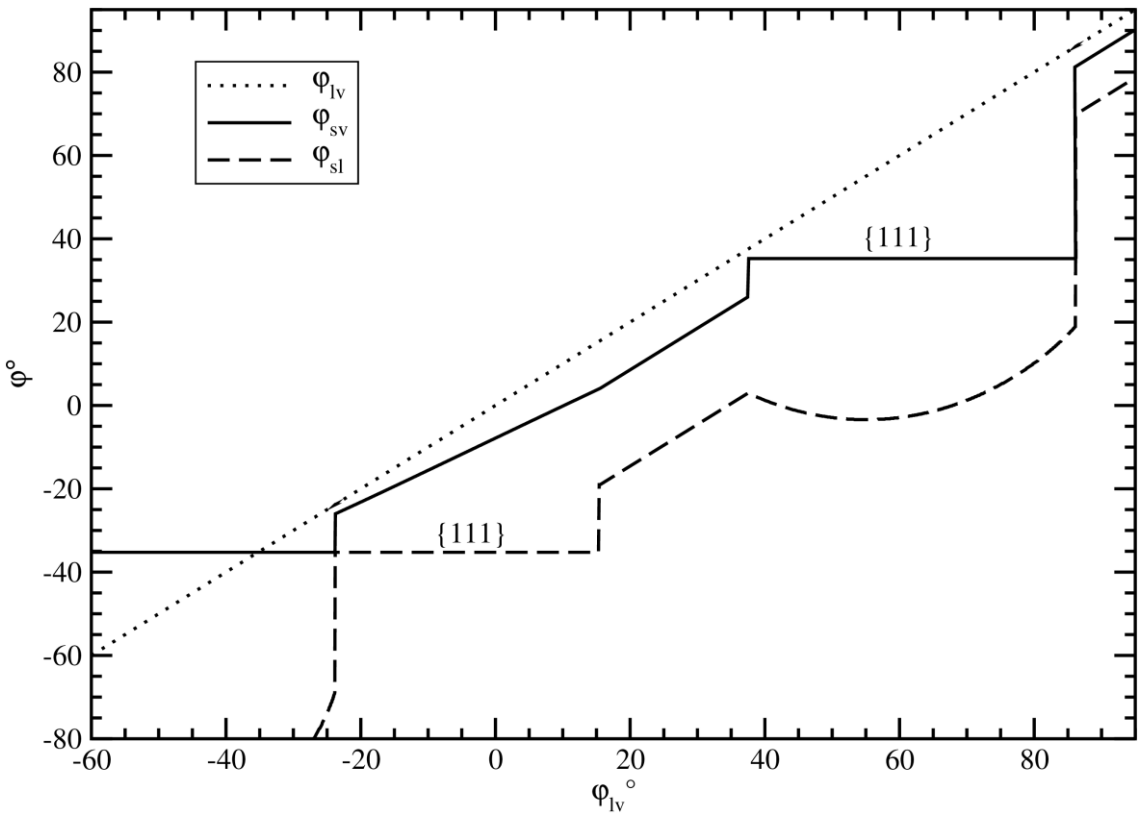

Figure 10: The angular diagram for [100] silicon crystal growth found from the equilibrium shapes of interfaces. It shows the equilibrium orientation in {110} plane of all interfaces at the TPL as function of meniscus free melt surface orientation.

In order to apply the diagram to the silicon crystal growth further consideration might be necessary. According to V. Voronkov [**Error! Reference source not found.**], the undercooling of the melt needed to sustain the growth of internal {111} facets leads to the bending of the external surface at the nanoscale. The equilibrium orientation of the external surface at TPL becomes different from the macroscopically observed orientation, Eq. (2). For the silicon crystal growth, the value of ϕ_{sv} could increase by about 20^{o} [**Error! Reference source not found.**] leading to outward bulging of the external surface and formation of growth ridges. That would shift upwards the parts of the angular diagram describing macroscopic orientation of the crystal external surface corresponding to growth with an internal {111} facet.

In conclusion, we obtained {110} cross-section of equilibrium shape of a silicon nanowire from molecular dynamics calculation. The shape is in good agreement with the experimental observations of Eaglesham et al [Eaglesham et al.Eaglesham, White, Feldman, Moriya, and Jacobson]. Confidence in the obtained shape allowed us to construct the angular diagram that shows the orientation of the internal and external surface of a silicon crystal on the orientation of the free melt surface at TPL. The obtained diagram agrees well with our understanding of silicon crystal growth parameters. We do not know any other example where such a diagram has been obtained using quantitative data. The diagram can be used to describe the silicon crystal growth from a melt. The approach is extendable to the growth of other crystalline materials. It is systematically improvable by obtaining better interatomic interaction potentials and by running larger molecular dynamics calculation.

References

[Duffar] T. Duffar, Crystal Growth Processes Based on Capillarity: Czochralski, Floating Zone, Shaping and Crucible Techniques, John Wiley & Sons, 2010.

[Fritzler et al.Fritzler, Trukhanov, Kalinin, Smirnov, Kolesnikov, and Vasilenko] K. Fritzler, E. Trukhanov, V. Kalinin, P. Smirnov, A. Kolesnikov, A. Vasilenko, In situ monitoring of floating-zone-grown si(111) crystal structure using the behavior of ridgelike protrusions, Technical Physics Letters 33 (2007) 521–523.

[Ciszek] T. Ciszek, Non-cylindrical growth habit of float zoned dislocation-free [111] silicon crystals, Journal of Crystal Growth 10 (1971) 263–268.

[Tiller] W. Tiller, The Science of Crystallization: Microscopic Interfacial Phenomena, Cambridge University Press, 1991.

[Voronkov 1978] V. V. Voronkov, Mass Transfer at the Surface of a Crystal Near to Its Boundary With the Melt, and its Influence on the Shape of the Growing Crystal, Sov. Phys. Crystallogr. 23 (1978) 137–141.

[Voronkov 1983] V. V. Voronkov, The faceting of crystals pulled from a melt, Akademiia Nauk SSSR Izvestiia Seriia Fizicheskaia 47 (1983) 210–218.

[Voronkov 1985] V. V. Voronkov, The effect of the faceting of the crystallization front on the external shape of crystals, Akademiia Nauk SSSR Izvestiia Seriia Fizicheskaia 49 (1985) 2467–2472.

[Herring 1951a] C. Herring, Surface tension as a motivation for sintering. In The physics of Powder Metallurgy. Edited by W.E. Kingston., McGraw-Hill Book Company, Inc., New York, 1951a.

[Herring 1951b] C. Herring, Some theorems on the free energies of crystal surfaces, Phys. Rev. 82 (1951b) 87–93.

[Voronkov 1980] V. V. Voronkov, , Akademiia Nauk SSSR Izvestiia Seriia Fizicheskaia 44 (1980) 226–235.

[Muller and Metois] P. Muller, J. Metois, Anisotropy of the surface thermodynamic properties of silicon, Thin Solid Films 517 (2008) 65 – 68.

[Eaglesham et al.Eaglesham, White, Feldman, Moriya, and Jacobson] D. J. Eaglesham, A. E. White, L. C. Feldman, N. Moriya, D. C. Jacobson, Equilibrium shape of si, Phys. Rev. Lett. 70 (1993) 1643–1646.

[Plimpton] S. J. Plimpton, Fast parallel algorithms for short-range molecular dynamics, http://lammps.sandia.gov/, J. Comp. Phys. 117 (1995) 1–19.

[Stillinger and Weber]F. H. Stillinger, T. A. Weber, Computer simulation of local order in condensed phases of silicon, Phys. Rev. B 31 (1985) 5262–5271.

[Weakliem and Carter] P. C. Weakliem, E. A. Carter, Constant temperature molecular dynamics simulations of Si(100) and Ge(100): Equilibrium structure and short-time behavior, The Journal of Chemical Physics 96 (1992) 3240–3250.

[Scheel and Fukuda] H. Scheel, T. Fukuda, Crystal Growth Technology, John Wiley & Sons, 2003.

[Apte and Zeng] P. A. Apte, X. C. Zeng, Anisotropy of crystal-melt interfacial free energy of silicon by simulation, Applied Physics Letters 92 (2008) 221903.

[Eustathopoulos et al.Eustathopoulos, Nicholas, and Drevet] N. Eustathopoulos, G. Nicholas, B. Drevet, Wettability at High Temperatures, Pergamon Materials Series, Elsevier Science, 1999.

[Wunscher et al.Wunscher, Ludge, and Riemann] M. Wunscher, A. Ludge, H. Riemann, Growth angle and melt meniscus of the RF-heated floating zone in silicon crystal growth, Journal of Crystal Growth 314 (2011) 43 – 47.

[Satunkin] G. Satunkin, Determination of growth angles, wetting angles, interfacial tensions and capillary constant values of melts, Journal of Crystal Growth 255 (2003) 170 – 189.

[Surek and Chalmers] T. Surek, B. Chalmers, The direction of growth of the surface of a crystal in contact with its melt, Journal of Crystal Growth 29 (1975) 1 – 11.

Projekta zinātniskais vadītājs Dr.Phys. Jānis Virbulis